Finite-Element Modelling of Magnetic Material Degradation Profiles due to Punching

Madeleine Bali[1], Herbert De Gersem[2], and Annette Muetze[1]
[1]Graz University of Technology, Inffeldgasse 18, 8010 Graz, Austria, madeleine.bali@tugraz.at
[2]KU Leuven Kulak, Etienne Sabbelaan 53, 8500 Kortrijk, Belgium, herbert.degersem@kuleuven-kulak.be

***Abstract*—Different profiles of magnetic material degradation due to punching are considered in electromagnetic finite element modelling of electric machines. Linear, polynomial, and exponential decrease of the relative permeability towards the cut edge are distinguished. The method and its implementation are presented. An example application is given for illustration purposes.**

***Index Terms*—Degradation, electric machines, finite element methods, magnetic cores, punching, soft magnetic materials.**

I. Introduction

The lamination sheets of the cores of electric machines are typically obtained through punching from the original coils of steel sheets. The punching process degrades the magnetic properties of the steel (e.g. [1], [2]) and is commonly found to have the most significant degrading effect of all manufacturing steps (e.g. [3], [4]).

The degradation process itself and its influence on the magnetic properties of the final sheets used in the assembled machines are very complex to understand and to model. Furthermore, a variety of types of electric steel materials is used and the different alloys show different deterioration behaviour during cutting. Detailed finite-element (FE) analyses of the mechanical stress on the steels mechanical and subsequently magnetic properties have been carried out ([5], [6]).

We consider such steel degradation in the *electromagnetic* FE modelling of electric machines with the relative permeability decreasing towards the edge according to a prescribed profile. Linear, polynomial, and exponential decrease are distinguished. Degradation depth, degree of degradation, and profile coefficients can be adjusted to account for different factors of influence, such as material alloy and details of the cutting process.

II. Simulation Procedure

A particular calculation procedure is set up (Fig. 1) to determine the effect of local material degradation on the magnetic field distribution within an electric machine. The material degradation is implemented as an inhomogeneous material distribution. The magnetic field is calculated from a 2D nonlinear magnetostatic FE formulation [7]. The magnetic field distribution within the stator core is studied for a given air-gap flux level ϕ. Change of machine performance parameters such as magnetic reluctance, required MMF, as well as iron loss density and total iron loss are computed subsequently.

The spatial distribution of the heavily nonlinear magnetic material characteristic is represented by the *degradation profile* $\gamma(s)$ representing the relative decrease in permeability according to the distance $s(x, y)$ between the considered material point (x, y) and the nearest cut edge. The degradation profile $\gamma(s) \in]0, 1]$ decreases from 1 far inside the material to the *degradation factor* $\hat{\gamma}$ at the cut edge. Notice that $\hat{\gamma} = 1$ corresponds to the reference situation where punching does not have any effect. The shortest distance for which $\gamma(s) = 1$ is referred to as *degradation depth* δ.

For linear material, the influence of the plastic strain causes a decrease of the permeability $\mu_{\mathrm{Fe,li}}$, to $\mu^{\star}_{\mathrm{Fe,li}} = \gamma(s)\mu_{\mathrm{Fe,li}}$, where * denotes the characteristic after the punching process.

Experiments for nonlinear materials indicate that the magnetic flux density at which saturation starts to occur is marginally influenced by the plastic strain [5]. Therefore, the decrease in permeability is modelled by an increase of the magnetic field strength by the factor $1/\gamma(s)$. When the BH-characteristic of the non-deteriorated material is given by a set of data points $(B_i, H_i)|_{\mathrm{nl}}$, $i = 1, \ldots, n$, then, the BH-characteristic of the deteriorated material becomes $(B_i, H_i)|^{\star}_{\mathrm{nl}} = (B_i, H_i)|_{\mathrm{nl}}/\gamma(s)$.

The magnetic field in the air-gap of rotating field machines has a sinusoidal spatial distribution. For machines with a translational symmetry, the air-gap field can be described

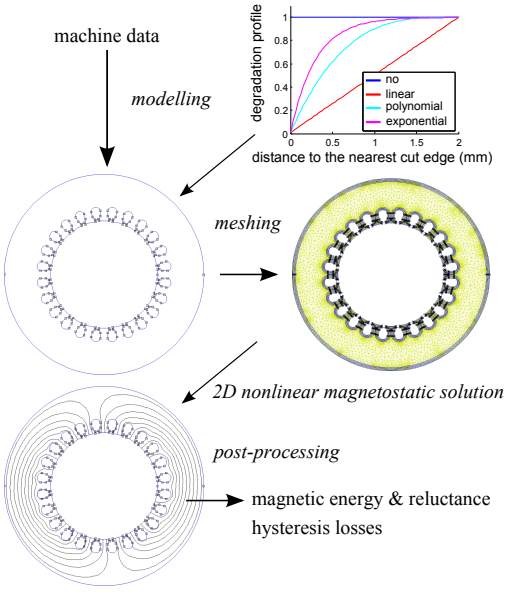

Fig. 1. Calculation procedure (modelling, meshing, FE solution, and post-processing).

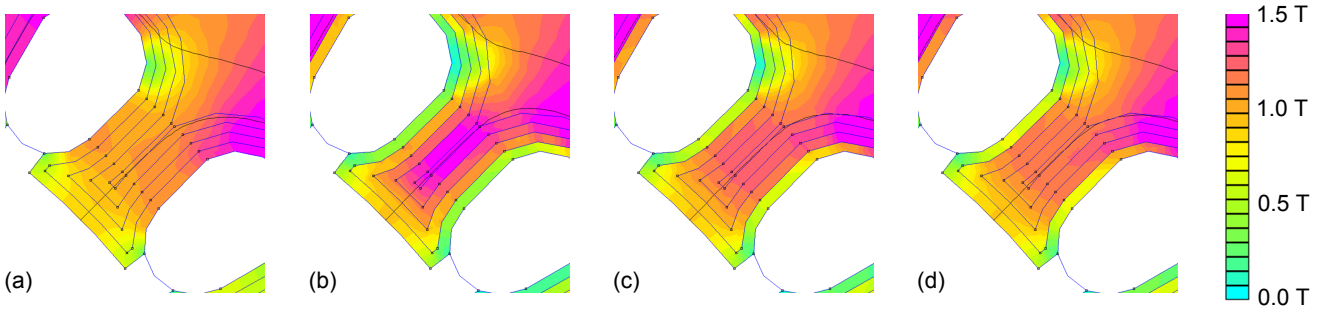

Fig. 2. Simulated distribution of the magnetic flux density for (a) reference situation: material not affected by punching and three different types degradation profiles with $\hat{\gamma} = 0$ and $\delta = 2\,\mathrm{mm}$: (b) *linear* degradation profile, (c) *polynomial* degradation profile, $q = 3.3$, (d) *exponential* degradation profile, $\delta_s = 0.3$.

by the z-component of the magnetic vector potential $A_z = \hat{A}_z \cos(p\theta - \varphi)$, where p is the pole-pair number, θ the azimuthal coordinate, and φ the phase constant at the considered time instant. The total flux coupled with the machine windings is $\phi = \hat{A}_z \ell_z$, where ℓ_z is the machine length. The magnetic flux closes through the laminated stator core and experiences a reluctance R_m.

A 2D FE model is created by scripting the FEMM software [8] (Fig. 1). The mesh is constructed by the Triangle software [9] embedded in FEMM. The degradation profile is discretised by piecewise constants at a number of boundary layers along the cut edges (Fig. 1). Each layer is associated with a different, appropriately scaled BH-characteristic. The air-gap field distribution is applied by assigning fixed values $\frac{\phi}{\ell_z}\cos(p\theta_i)$ to the inner boundaries of the slots. θ_i denotes the azimuthal position of the centre of slot i. The nonlinear magnetostatic solver of FEMM is invoked and the magnetic field distribution within the yoke is computed.

III. Degradation Profiles

Three degradation profiles $\gamma(s)$ are distinguished (Fig. 1):

1) Linear profile:

$$\gamma(s) = \frac{1-\hat{\gamma}}{\delta} s + \hat{\gamma} \tag{1}$$

2) Polynomial profile:

$$\gamma(s) = 1 - (1-\hat{\gamma}) \left(\frac{\delta - s}{\delta}\right)^q , \tag{2}$$

where q is a (positive, real) exponent determining the decay rate of the degradation.

3) Exponential profile:

$$\gamma(s) = 1 - (1-\hat{\gamma}) e^{-\frac{s}{\delta_s}} , \tag{3}$$

where δ_s is the degradation skin depth. (Depth where the effect of degradation has been reduced to one third.)

A sufficient resolution of the degradation layers in the FE mesh is of paramount importance. Especially for polynomial and exponential profiles with large exponents or small degradation skin depths respectively the mesh density has to be specified carefully. Notice that a thin layer description as is typically done for thin eddy-current layers [10] is not applicable here, since the flux is pushed away from the cut edge. The most promising technique for increasing the modelling accuracy is the introduction of a supplementary space of approximation functions with higher order resolution perpendicular to the cut edge [11].

IV. Application

The proposed simulation approach is applied to the yoke of a $0.75\,\mathrm{kW}$ capacitor motor (Fig. 1). A two-pole magnetic flux path through the stator yoke is considered. The yoke is slightly saturated and thus within the operating region where degradation is most important [3].

The detailed views of the simulated magnetic flux density distributions (Fig. 2) show that the reduced permeability at the cut edges forces a larger part of the flux to flow through the centre parts of the teeth which increases the maximum occurring flux densities: For the linear case, the latter increases by approximately 50%, for the polynominal and exponential degradation profiles the increase is in the order of 30%. (All for degradation depths of almost half of the width of the tooth and maximum degradation factor $\hat{\gamma} = 0$.) The reluctance R_m increases by 41, 14, and 9% respectively.

References

[1] E.G. Araujo, J. Schneider, K. Verbeken, G. Pasquarella, and Y. Houbaert, "Dimensional effects on magnetic properties of Fe-Si steels due to laser and mechanical cutting," *IEEE Trans. Magn.*, vol. 46, no. 2, pp. 213–216, Feb. 2010.

[2] A. Schoppa, H. Louis, F. Pude, and C. von Rad, "Influence of abrasive waterjet cutting on the magnetic properties of non-oriented electrical steels," *J. Magn. Mag. Mat.*, vol. 254-255, pp. 370–372, Jan. 2003.

[3] A. Schoppa J. Schneider, and C.D. Wuppermann, "Influence of the manufacturing process on the magnetic properties of non-oriented electrical steels," *J. Magn. Mag. Mat.*, vol. 215-216, pp. 74-78, June 2000.

[4] Y. Kurosaki, H. Mogi, H. Fujii, T. Kubota, and M. Shiozaki, "Importance of punching and workability in non-oriented electrical steel sheets," *J. Magn. Mag. Mat.*, vol. 320, no. 20, pp. 2474–2480, Oct. 2008.

[5] F. Ossart, E. Hug, O. Hubert, C. Buvart, and R. Billardon, "Effect of punching on electrical steels: Experimental and numerical coupled analysis," *IEEE Trans. Magn.*, vol. 39, no. 5, pp. 3137–3140, Sep. 2000.

[6] K. Fujisaki and S. Satou, "Numerical Calculations of electromagnetic fields in silicon steel under mechanical stress," *IEEE Tr. Magn.*, vol. 40, no. 4, pp. 1820-1825, July 2004.

[7] J.P.A. Bastos and N. Sadowski, *Electromagnetic Modeling by Finite Element Methods*, Marcel Dekker, Inc., New York, Basel, 2003.

[8] Finite Element Method Magnetics (FEMM), *www.femm.info*

[9] J.R. Shewchuk, "Delaunay refinement algorithms for triangular mesh generation," *Computational Geometry*, vol. 22, no. 1-3, pp. 21–74, May 2002.

[10] S. Barmada, L. Di Rienzo, N. Ida, and S. Yuferev, "Time domain surface impedance concept for low frequency electromagnetic problems - Part II: Application to transient skin and proximity effect problems in cylindrical conductors," *IET Science, Measurement & Technology*, vol. 152, no. 5, pp. 207-216, Sep. 2005.

[11] I. Tsukerman, "Electromagnetic applications of a new finite-difference calculus," *IEEE Trans. Magn.*, vol. 41, no. 7, pp. 2206-2225, Jul. 2005.